Fen Bilimleri Dergisi, 26(2) (2014) 47-55.
Marmara Üniversitesi

http://dx.doi.org/10.7240/MJS.2014267516

MULTIDIMENSIONAL MODELING OF COMPRESSED BIO GAS (CBG) ENGINE FOR ULTRA LOW EMISSION

Hasan Köten[1*], Zafer Gül[1]
[1]Department of Mechanical Engineering, Marmara University, 34722, Kadikoy, Istanbul, Turkey. hasan.koten@marmara.edu.tr zgul@marmara.edu.tr

Abstract- The purpose of this study is to find out in-cylinder flow characteristics of a four-cylinder, 2,3 liter diesel engine before the fuel injection and also properly simulate the atomization process in order to improve the combustion efficiency and emission parameters. A complete intake stroke with Compressed Bio Gas (CBG) port injection, compression stroke, pilot fuel injection at the end of the compression and exhaust stroke simulated in 3D. Both naturally aspirated and turbo-charged modes of operations were studied. In this study, cold flow structure, fuel atomization for different spray models and dual fuel combustion are investigated. A comprehensive model for atomization of liquid sprays under high injection pressures has been employed. Finally, a calculation on an engine configuration with compression, spray injection and CBG-diesel combustion in a direct injection dual fuel diesel engine is presented. In 3D CFD study, selected proper cases modeled using full geometry of diesel engine. Fine grids were tested with 1,700,000 hexahedral cells. In this paper, fine grid results are evaluated. CBG fuel induced during intake process in dual fuel diesel combustion engine and then mixed with air before the premixed gas enters the cylinder. It is ignited by the injection of pilot diesel fuel near the Top Dead Center (TDC). This lean combustion and diluted gas mixture cause low in-cylinder temperature and resulting in a NOx emission. The results are in agreement qualitatively with the previous studies in the literature.

Key Words- CFD, dual-fuel, biogas, cold flow, spray, combustion modelling, emission.

1. INTRODUCTION

In transport industry, compression ignition (CI) engines are highly preferred as power supply compared to spark ignition (SI) engines due to their high thermal efficiency, perfect fuel economy and low regular emissions of unburned hydrocarbon (HC), carbon monoxide (CO) and carbon dioxide (CO_2). However, from environmental point of view, diesel engines commonly exhaust a higher amount of particulate matter (PM) and nitrogen oxide (NOx) pollutant emissions compared to exhaust emission properties of gasoline engines [1,2]. Throughout the recent years, the fossil-fuels have damaged from a certain rise in prices of petroleum fuels because of the limitations of deposit, supply and significantly increase in desire of petroleum fuels resulting from the industrialization. In addition to the strengthening of the regulations for PM and NOx emissions from diesel motors and reductions in CO_2, that is a greenhouse gas, also caused important problems for environment [3,4]. Therefore, bio-fuels (liquid and gaseous) have been commonly used for intensive research studies all over the world because they are overestimated impressively alternative fuels. Bio-fuels like biogas (gaseous fuel) is renewable, parsable biologically and is the most promising alternative fuels for diesel motors. Biogas is obtained after the result of a fermentation process with renewable agricultural supplies like animal fats, waste oils and organic waste. The main advantages of biogas are its reducing the formation of CO, HC and PM emissions during the combustion because of that it has low carbon inside methane, low particulate content, and includes hydrogen-containing compounds [5,6]. Usually, biogas is produced by the anaerobic fermentation of organic waste in landfills and the anaerobic digestion of sludge, crops, and agro-industrial products and animal organic waste [7]. The main component (generally about

*Corresponding Author : Hasan Koten, hasan.koten@marmara.edu.tr

over 65% by vol.) of the biogas is methane (CH4). Engines with low compression ratios can use fuels with lower octane numbers, but high-compression engines must use high-octane fuel to avoid self-ignition and knock. It exhibits greater resistance to the knock phenomenon due to its higher auto-ignition temperature and octane rating. It is important that the temperature at the beginning of combustion for diesel cycle be low enough so that self-ignition and knock do not become problems [8,9].

Mustafi et al. experimentally investigated the exhaust emission characteristics of a direct injection (DI) diesel engine operated with gas main or gas-diesel dual-fuels [10]. Their study showed that stable engine operation may be possible with natural gas (NG) and biogas fueling without any modifications to either the engine or its operation, and that the PM (about 70% by mass) and NOx emissions (more 37% by mass) of duel-fueling tend to be small compared to the ones from diesel fueling operating under the same operation. Maji et al. investigated the use of compressed natural gas (CNG) in lessening the noise level, specific fuel consumption, and NOx emissions, however, the UHC increased inside the dual-fuel mode having a substitution of CNG for 75% of the diesel fuel [11]. Shen et al. investigated the influence in the CNG ratio, the advance of the pilot injection for diesel fuel and also the intake temperature around the combustion process, emissions, and engine performance of a dual-fueled engine [12, 13].

2. MATHEMATICAL MODELING

2.1 Governing Equations

The equations employed to describe mass, momentum and energy conservation equations and the turbulence model for high Reynolds number in flux vector notation under working conditions can be expressed as:

$$\frac{\partial \rho_l}{\partial t} + \nabla.(\partial \rho_l u_l) = \frac{\dot{m}_{imp}}{h}$$

$$\frac{\partial}{\partial t}(\rho_l u_l) + \nabla.(\rho_l u_l u_l) = -\nabla p_l + \rho_l g + \nabla.\tau_l + s_{imp}\delta(\xi - h)\,\frac{\partial}{\partial t}(\rho_l h_l) + \nabla.(\rho_l u_l h_l) = \nabla.(k_l \nabla T_l) + \frac{\dot{Q}_{imp}}{h}$$

$$\tau_k^t = \mu_k^t\left(\nabla u_k + (\nabla u_k)^T + \left(-\left(\frac{2}{3}\nabla.u_k\right)\right)I\right) - \frac{2}{3}\rho_k k_k I$$

2.2 Turbulence Models

Two-equation, k-ε models are commonly used for engineering predictions of turbulent flows to provide computational expediency and ease of implementation in finite-volume numerical codes. Their accuracy is generally acceptable only for prediction of mean flow quantities. In particular, the standard k-ε model of Launder and Spalding (Launder and Spalding, 1974) has been criticized by many researchers as being inaccurate for prediction of re-circulating flows and complex shear layers, due to its over dissipative nature. In an attempt to improve the predictive ability of the standard k-ε models, a number of alternatives have been offered. Among them the RNG k-ε model (Yakhot and Orszag, 1986, 1992), anisotropic k-ε model of Speziale(Speziale, 1987), Morel & Mansour version of the k-ε model(Morel & Mansour, 1982), and the k–ω model of Wilcox (Wilcox,1998) are well known. Gul (Gul, 1994), has also offered a three-equation turbulence model in order to predict the compressed turbulence in IC engines.

In this work various turbulence models including the Chen's k-ε model (Chen and Kim, 1987) have been tested and the RNG k-ε model has been chosen for the rest of the simulations.

2.3 Spray Models

Huh's model (Huh and Gosman, 1991) was used as an atomization model in the simulations. This model is based on the premise that the two most important phenomena in spray atomization, the gas inertia and the internal turbulence stresses generated in the nozzle. This situation can be introduced in two steps.

The average turbulent kinetic energy, k_a and its dissipation rate at the hole exit can be shown as follows, according to Huh's atomization model:

$$k_a = \frac{U^2}{8\frac{L}{D}}\left(\frac{1}{c_d^{\,2}} - K_c - 1\right), \qquad \varepsilon_a = \frac{K_\varepsilon U^3}{2L}\left(\frac{1}{c_d^{\,2}} - K_c - 1\right)$$

where U is the average injection velocity over the time period of injection, L and K_c are the hole length and form loss coefficient, K_ε is an empirical coefficient and c_d is the nozzle's discharge coefficient.

The initial values of the turbulence length and time scales can be shown as:

$$\left[l_t^0 = C_\mu^{0.75}\frac{k_a^{1.5}}{\varepsilon_a}; \tau_t^0 = C_\mu^{0.75}\frac{k_a}{\varepsilon_a}\right]$$

The fuel particles may become unstable due to the interfacial forces acting on their surfaces during the relative motion according to the continuous phase. This problem was solved by using the break-up model of Reitz and Diwakar (Reitz and Diwakar, 1986). Droplet break-up due to aerodynamic forces exists in two modes in Reitz and Diwakar model. First one is 'Bag break-up' (Reitz and Diwakar, 1986), in which the non-uniform pressure field around the droplet causes it to expand in the low-pressure wake region and eventually disintegrate when surface tension forces are overcome. This model provides to explain the effects of the change on discrete phase, when the droplet temperature reaches the boiling or critical temperature. The following conditions are considered:

1. $T_d \geq T_c$

Here, T_c is the critical temperature, i.e. the temperature at which

$$\left(\frac{\partial \rho}{\partial V}\right)_{T_c} = 0$$

2. $T_d \geq T_b(p_t)$

Here, T_b is the boiling temperature at the ambient pressure. The boiling temperature is defined by the temperature at which the pressure of saturation, P_s, balances the gas pressure. For the first condition, the droplet evaporates suddenly. And if the second condition satisfied, then mass transfer rate can be introduced as follows:

$$\frac{dm_d}{dt} = \frac{-2\pi k D_d}{c_p}(1 + 0.23\,\mathrm{Re}^{0.5})\ln\left[1 + \frac{c_p(T - T_d)}{h_{fg}}\right]$$

where k is the conductivity and c_p the specific heat of the mixture. During the boiling droplet temperature is constant. Then, the rate of the heat transfer from droplet to the continuous phase can be introduced as follows:

$$\dot{q}_g = -h_{fg}\frac{dm_d}{dt}$$

Bai's (1995) Spray impingement model was used in the simulations as a wall-interaction model for discrete phase. This model was formulated within the framework of the Lagrangian

model, which is based on literature findings and mass, momentum and energy conservation constraints. The complete model formulation distinguished between dry and wetted wall impingement and is applicable to wall temperatures that are less than the liquid boiling or critical temperature.

2.4. Combustion model

Wiebe function for 1D approximation and Extended Coherent Flame Model (ECFM) for 3D CFD solution are used to carry out Combustion modeling. The Wiebe function can be expressed follows.

$$x_b = 1 - \exp(-a(\frac{\theta - \theta_0}{\Delta\theta})^{m+1})$$

Where x_b is the mass fraction burned, θ is the crank angle, θ^0 , which fixes the timing is the crank angle at the start of combustion, a and Δθ are adjustable constants that determine the combustion duration and m is an adjustable parameter that fixes the shape of the combustion progress curve. ECFM (Duclos et. al., 1999) and the 3-Zone ECFM (ECFM-3Z) broadly belong to the Coherent Flame Model (CFM) family, but are extended to non-homogeneous turbulent premixed and unpremixed (diffusion) combustion. In the ECFM3Z combustion model, the state of the gases mixture is defined in the 2D space. It is simultaneously described in terms of mixing and progress of reaction as schematically represented in Figure 1(Colin and Benkenida, 2004).

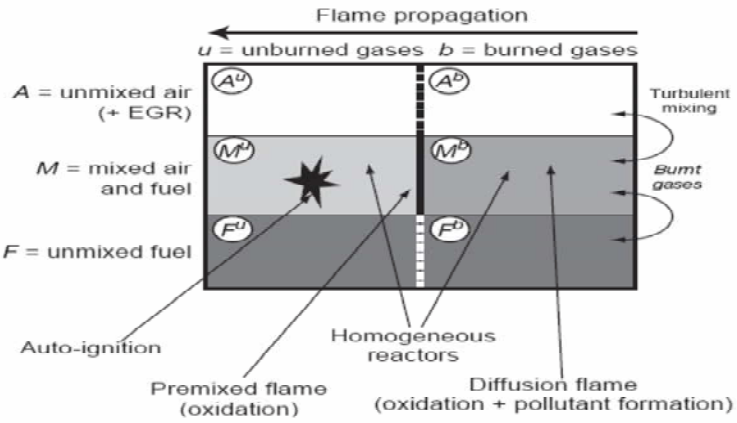

Figure 1. Schematic of the ECFM3Z model computational cell.

3. NUMERICAL METHODOLOGY and MESH GENERATION

The AVL boost and CFD code based on finite volume method has been utilized to solve the discretized continuity and Navier-Stokes equations. The code has the capability of solving the transient, compressible, turbulent-reacting flows with sprays on the finite volume grids with moving boundaries and meshes. Fully hexahedral meshes are utilized for entire solution due to the requirements of moving mesh. Piston and valve motion are carried out by cell activation and deactivation and supported by vertex motion routines supplied. The module is competent for handling the complex geometry and enabling the computational domain includes the intake and exhaust ports, valves and the combustion chamber with moving boundary. Governing equations along with the a number of turbulence model equations were solved to compute the flow field, temperature distribution and the turbulence properties by using Monotone Advection and Reconstruction Scheme (MARS) and Pressure Implicit

Splitting of Operator algorithm (PISO) with 0.1°CA time step size. Analysis of these results showed the swirl of the flow field in the combustion chamber.

3.1 Moving Boundaries

CFD module is used to define the piston movement, intake and exhaust valve lifts. It has been exploited to generate the grid to create the hexahedral cells for the engine model. The computational domain includes the intake ports and valves, the cylinder head and piston bowl as shown in Figure2. The number of cells changes from 500.000 cells in TDC and over a million cells in BDC, where about of the cells used to generate the mesh at the cylinder head, intake and exhaust ports and piston bowl in the case of considering the mesh quality and reasonable computational cost. For the mesh generation hexahedral cells have been accepted because they provide a better accuracy, stability and less computer run time compared to tetrahedral cells.

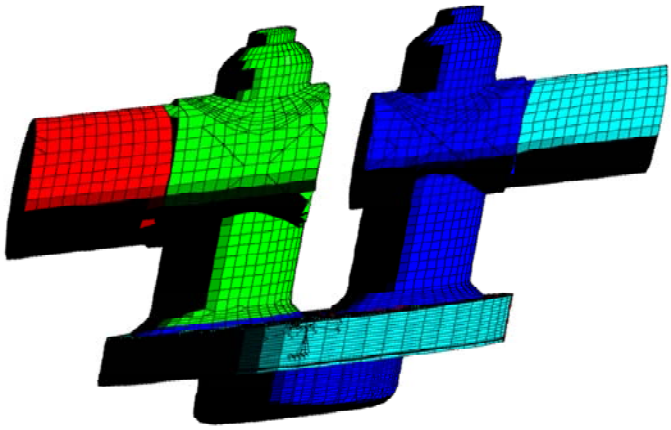

Figure 2. The moving mesh and boundary at 20 °CA aTDC.

The notion of moving mesh is that the cell is squeezed to zero volume over one time step, with all its contents (pressure, temperature, mass, momentum, enthalpy, etc.) being expelled into the neighboring cells. Hence, conservation is satisfied exactly even with removal of any cell layer. At the same time, when the cell layers are added, they increase from zero size to their full volume, absorbing the conserved variables through their faces.

3.2 Equation Discretization and Algorithms

The numerical approximation and computation is based on the pressure-correction method and the PISO algorithm. The second order upwind differencing scheme (MARS) as the spatial discretization is employed for the momentum, energy and turbulence equations. The temporal discretization is the implicit method, with constant time step. There are high local velocities in

the discharge zone and at the beginning and the end of the intake stroke, when the valve lift is quite small. Hence, the time step must be small enough as 0.1 °CA (on computation) in order to succeed the stability criterion (Versteeg and Malalasekera, 1995). The running calculations started when intake valve opening and continued to the 20 °CA aTDC with the fuel injection. After that pressure and temperature values for engine set the boost pressure and temperature in according to operating speed varies from 600 to 2200 rpm under naturally aspirated and turbo charged conditioning. Turbulence initialization was set at 'k-ε constant' and default values were selected for energy and dissipation, which is quite sufficient for fully turbulent fluid flow. Constant pressure boundary conditions were carried out at both intake and exhaust ports so that the dynamics effects were omitted. The walls of the intake and exhaust ports and the lateral walls of the valves were considered as the adiabatic condition. The constant temperature boundary conditions were allocated independently for the cylinder head, the cylinder wall, and the piston crown that outline the walls of the combustion chamber. The temperature on each of these walls will be calculated numerically in the form of iteration for every time step automatically.

4. RESULTS AND DISCUSSIONS

In figure 3 In-cylinder emission results according to mass fraction at different crank angles are depicted. Results show that 1-D and 3-D analysis gives similar characteristics in early combustion steps for all emission values. But, CO amount decreases in 1-D analysis while increases in 3-D about 5° CA aTDC. As can be seen in Figure 3 NO_x amounts results behave similar in all combustion steps and slowly increases.

In-cylinder 3D CFD results pressure value reaches maximum value about 1 °CA aTDC but 1D analysis reaches a few degree crank angle more than that of the previous case, (about 5 °CA aTDC, figure 4). Similarly, 3D CFD temperature results reach maximum value at about 3 °CA aTDC and 1D analysis yields a maximum about 20 °CA aTDC. It is shown that a few difference between 1D and 3D CFD analysis results. This is possibly due to the injection parameters chosen for CFD calculation (i.e. maximum droplet and parcel number)

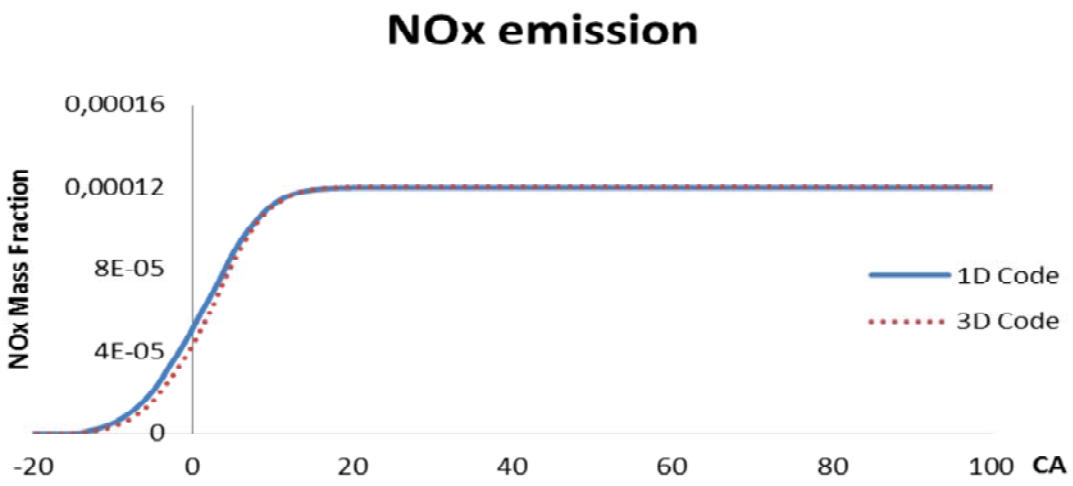

Figure 3. In-cylinder NOx mass fraction results

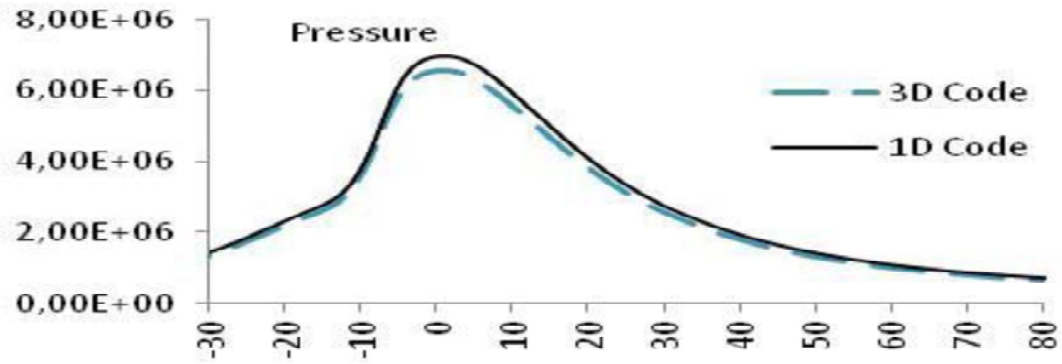

Figure 4. In-cylinder pressure results during combustion process.

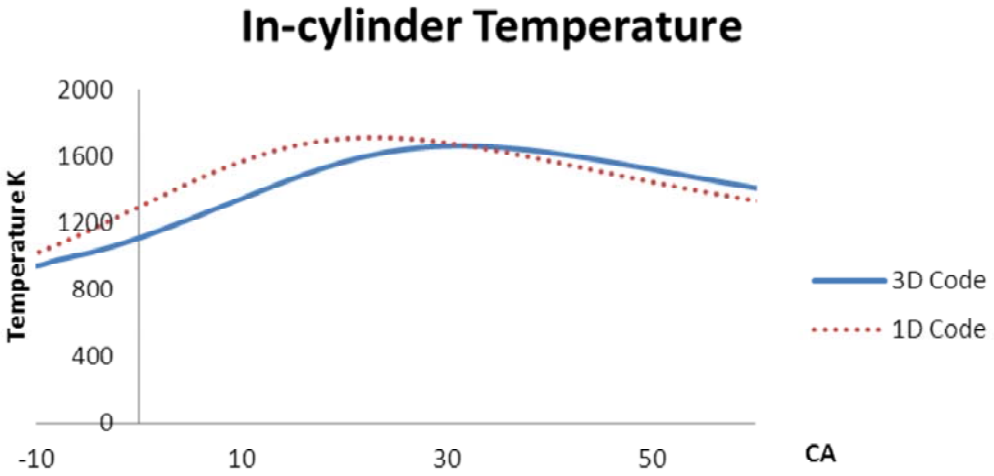

Figure 5. In-cylinder temperature results.

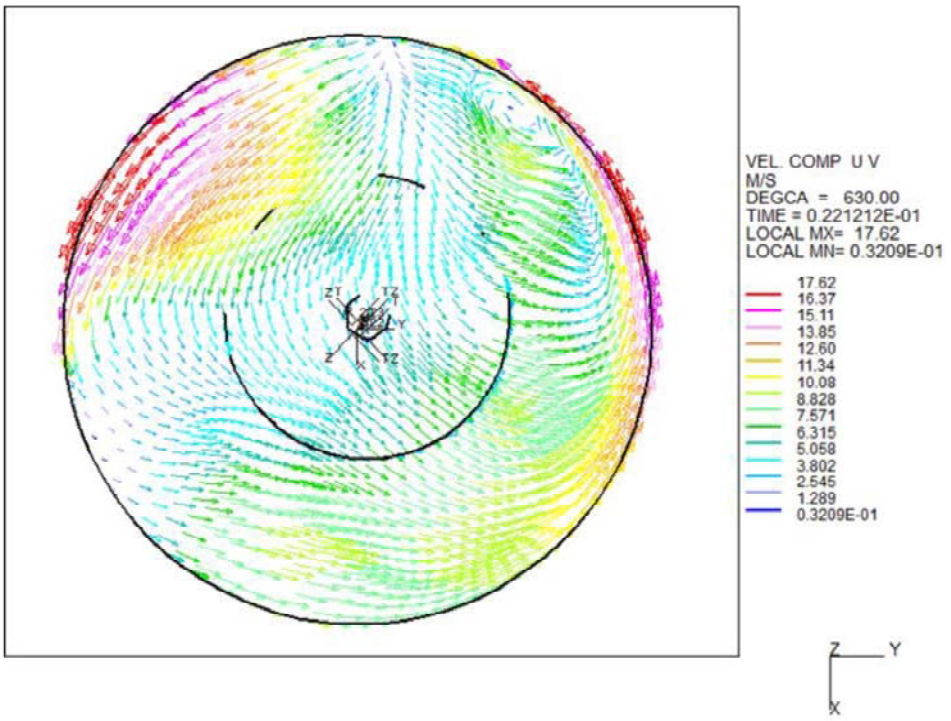

Figure 6. Velocity vector field perpendicular to the vertical axis at 0.16mm below from cylinder head, 20 °CA aTDC.

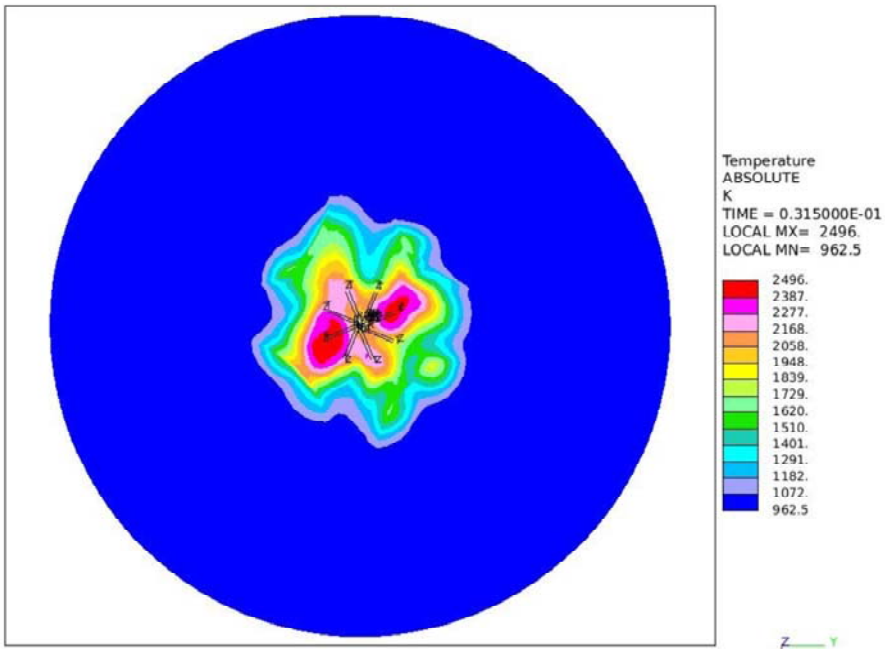

a) 10 °CA bTDC

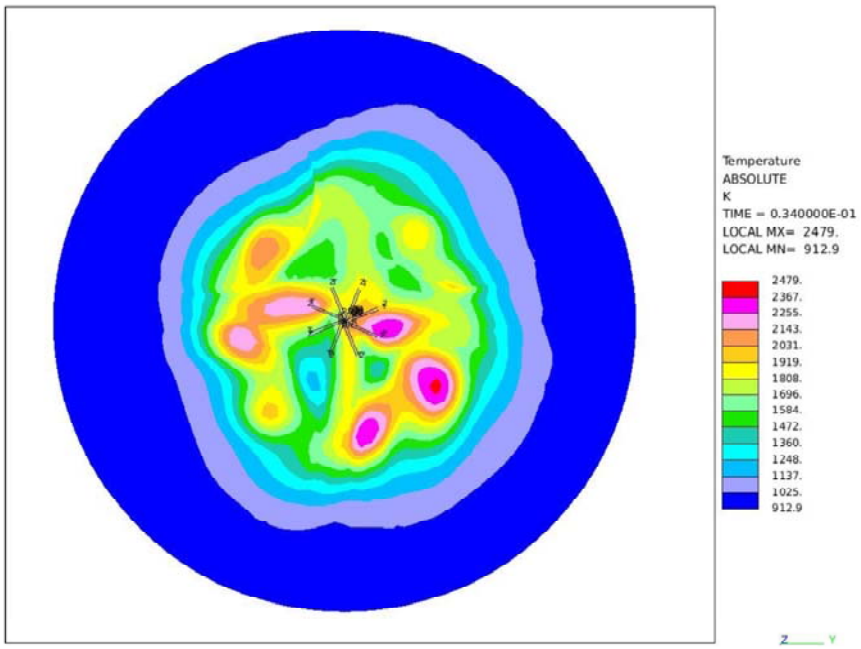

b) 20 °CA aTDC

Figure 7. Temperature contours perpendicular to the vertical axis at 0.16 mm below from cylinder head

As can be seen in Figure 6, there is an increase at velocity vector magnitude while piston moving to the TDC. That is because of flow motion from piston crown to the cylinder bowl (squish) and fuel injection. That also increases the turbulence level. Average in-cylinder temperature is about 1200 K for the combustion process while higher temperatures (2585° K locally) at earlier combustion steps can be seen in Figure 7.

5. CONCLUSIONS

In this project, user defined code is used to identify CBG and diesel fuels as leading reactant also a new combustion model (ECFM-3Z) is used successfully. Calculation on an engine configuration with intake, compression, spray injection, early combustion and exhaust in a DI Diesel engine is accomplished. Effect of in-cylinder design parameters in a DI diesel engine is investigated and presented. It is seen that results are widely in agreement qualitatively with the previous experimental and computational studies in the literature. CBG fuel is induced from intake port, mixed with fresh air and CBG-air mixture is ignited by pilot dodecane diesel fuel near TDC. Further study is needed to find the optimum engine parameters to bridge the gap between multidimensional and zero dimensional computations.

ACKNOWLEDGEMENTS

The authors would like to thank to Marmara University BAPKO Unit for supporting this research project under project no: FEN-C-DRP-101012-0327.

6. REFERENCES

1. S.H. Yoon, S.H. Park, C.S. Lee, Experimental investigation on the fuel properties of biodiesel and its blends at various temperatures, Energy and Fuels 22 (2008) 652–656.
2. R.L. McCormic, C.J. Tennant, R.R. Hayes, S. Black, Sharp, Regulated Emissions from Biodiesel Tested in Heavy Duty Engines Meeting 2004 Emission Standards, SAE 2005-01-2200, 2005.
3. M.Y. Kim, S.H. Yoon, C.S. Lee, Impact of split injection strategy on the exhaust emissions and soot particulates from a compression ignition engine fueled with neat biodiesel, Energy and Fuels 22 (2008) 1260–1265.
4. M.Y. Kim, S.H. Yoon, J.W. Hwang, C.S. Lee, Characteristics of particulate emissions of compression ignition engine fueled with biodiesel derived from soybean, Journal of Engineering for Gas Turbine and Power 130 (5) (2008) 052805-1–052805-7.
5. S.H. Park, S.H. Yoon, C.S. Lee, Effect of the temperature variation on properties of biodiesel and biodiesel–ethanol blends fuels, Oil & Gas Science and Technology 63 (6) (2008) 737–745.
6. S.H. Yoon, H.K. Suh, C.S. Lee, Effect of spray and EGR rate on the combustion and emission characteristics of biodiesel fuel in a compression ignition engine, Energy and Fuels 23 (2009) 1486–1493.
7. C. Rahmouni, M. Tazerout, O. Le Corre, A method to determine biogas composition for combustion control, SAE 2002-01-1708, 2002.
8. C. Tricase, M. Lombardi, State of the art and prospects of Italian biogas production from animal sewage: technical-economic considerations, Renewable Energy 34 (2009) 477–485.
9. B.B. Sahoo, N. Sahoo, U.K. Saha, "Effect of engine parameters and type of gaseous fuel on the performance of dual-fuel gas diesel engines-A critical review", Renewable and Sustainable Energy Reviews 13 (2009) 1151–1184.
10. N.N. Mustafi, R.R. Raine, A study of the emissions of a dual fuel engine operating with alternative gaseous fuels, SAE 2008-01-1394, 2008.
11. S. Maji, Amit Pal, B.B. Arora, Use of CNG and diesel in CI engines in dual fuel mode, SAE 2008-28-0072, 2008.
12. S. Jie, Q. Jun, Y. Mingfa, Turbocharged diesel/CNG dual-fuel engines with intercooler: combustion, emissions and performance, SAE 2003-01-3082, 2003.
13. Launder, B.E., and Spalding, D.B. 1974. 'The numerical computation of turbulent flows', Comp. Meth. in Appl. Mech. and Eng., 3, pp. 269-289.